



Original Article

The investigation of effects, signal pathways, and applications of high glucose on dental pulp stem cells



Shih-Yu Lee ^a, I-Hsun Li ^b, Wei-Cheng Tsai ^a, Ming-Hua Ho ^c,
Chung-Hsing Li ^{d,e*}

^a Graduate Institute of Aerospace and Undersea Medicine, National Defense Medical Center, Taipei, Taiwan

^b School of Pharmacy, National Defense Medical Center, Taipei, Taiwan

^c Department of Chemical Engineering, National Taiwan University of Science and Technology, Taipei, Taiwan

^d Division of Orthodontics, Pediatric Dentistry, and Special Needs Dentistry, Department of Dentistry, Tri-Service General Hospital, Taipei, Taiwan

^e School of Dentistry and Graduate Institute of Dental Science, National Defense Medical Center, Taipei, Taiwan

Received 16 March 2025; Final revision received 28 March 2025

Available online 12 April 2025

KEYWORDS

Dental pulp stem cells (DPSCs);
Mesenchymal stem cells (MSCs);
High glucose (HG);
Diabetes mellitus (DM);
Stem cell therapy

Abstract *Background/purpose:* Dental pulp stem cells (DPSCs) are among the most widely used dental-derived mesenchymal stem cells (MSCs), and their applications have involved various regions. The glucose metabolism plays a key role in cell function and the current literature presents conflicting evidence regarding the influence of glucose on MSCs' properties. This study evaluated the impact of high glucose (HG) on DPSCs.

Materials and methods: DPSCs were stimulated with indicated concentrations of glucose. Cell viability was assessed using a cell counting kit, while apoptosis and autophagy were analyzed via western blot. MSCs immunophenotypic properties were determined by flow cytometry. Osteogenic, adipogenic, and neurogenic differentiation potential were evaluated using western blot, Alizarin red staining, oil red-O staining, and morphological analysis.

Results: HG exposure led to a significant decrease in cell viability, with increased apoptosis and autophagy, as indicated by increased levels of cleaved caspase-3, cleaved poly (ADP-ribose) polymerase (PARP), and an elevated microtubule-associated protein 1 light chain 3 beta (LC3B)-II/LC3B-I ratio. However, the immunophenotypic characteristics of DPSCs remained unchanged. DPSCs also demonstrated enhanced osteogenic, adipogenic, and neurogenic differentiation potential by expressing Alizarin red and oil red-O staining,

* Corresponding author. School of Dentistry and Graduate Institute of Dental Science, National Defense Medical Center, No. 161, Sec. 6, Minquan E. Rd., Neihu Dist., Taipei City 11490, Taiwan.

E-mail address: chiyenchli@yahoo.com.tw (C.-H. Li).

neural-like cell morphology, and several differentiation-related proteins after HG culture stimulation.

Conclusion: The present study demonstrated that while HG slightly impairs DPSC viability, it promotes osteogenic, adipogenic, and neurogenic differentiation. Providing valuable insights into the mechanisms by which HG influences various differentiation pathways in DPSCs and establishes a foundation for potential clinical applications of DPSCs in regenerative medicine for diabetic patients.

© 2025 Association for Dental Sciences of the Republic of China. Publishing services by Elsevier B.V. This is an open access article under the CC BY-NC-ND license (<http://creativecommons.org/licenses/by-nc-nd/4.0/>).

Introduction

Stem cells are undifferentiated cells that exhibit self-renewal and multi-lineage differentiation capacity. They possess the capacity for extensive proliferative potential through numerous division cycles and can differentiate into specific tissues or organs in response to surrounding environmental cues, making them a fundamental component of regenerative medicine.^{1–3} Throughout development, embryonic stem cells (ESCs) give rise to tissue-specific adult stem cells that persist in various organs. These adult stem cells can regenerate portions of their resident tissues, making them a more ethically acceptable source of stem cells than ESCs. Mesenchymal stem cells (MSCs) are adult stem cells that can be isolated from various tissues and possess remarkable differentiation capacity and paracrine functions, enabling them to promote tissue repair and regeneration.⁴

Dental pulp is an innervated and vascularized loose connective tissue that originates from the neural crest. This tissue is rich in dental pulp stem cells (DPSCs), the most common form of dental-derived MSCs. DPSCs were first isolated and characterized by Gronthos et al. from human adult dental pulp tissue of the third molar tooth. They found that these cells shared similar properties to bone marrow-derived MSCs, including similar immunophenotype, clonogenic properties, capacity for self-renewal, etc.⁵ Previous studies have indicated that DPSCs expressed MSC-markers and can differentiate into multiple cell types, including odontoblasts, osteoblasts, adipocytes, and neural cells.^{6,7} More remarkably, DPSCs exhibit significant immunomodulatory properties, influencing cytokine secretion such as transforming growth factor-beta (TGF- β), interleukin (IL)-6, IL-10, and tumor necrosis factor-alpha (TNF- α) in immune cells, promoting anti-inflammatory responses while inhibiting pro-inflammatory cytokines.⁸ Small extracellular vesicles derived from DPSCs have also been shown to mediate macrophage phenotypes.⁹ These characteristics and ease of isolation and harvest make DPSCs valuable tools in regenerative medicine and immunotherapy, including neural tissue regeneration,¹⁰ bone tissue repair,^{11,12} periodontal disease treatment, etc.

Diabetes mellitus (DM), characterized by chronic hyperglycemia, is closely associated with a wide range of complications affecting multiple organs throughout the body, such as cardiovascular disease, skeletal disorders, and renal and ocular complications. Affecting approximately 422 million people globally in 2014,¹³ and it has been estimated

that the prevalence will increase by 10.1 % in 2030.¹⁴ Glucose transport and metabolism play crucial roles during mammalian development. Studies have shown that high glucose (HG) environments significantly impair the functionality of MSCs, such as altering mitochondrial dynamics, decreasing cell viability, increasing apoptosis,¹⁵ impairing osteogenic and neural differentiation potential,^{16,17} inducing reactive oxygen species (ROS) generation,¹⁸ and also affects immunomodulatory functions.¹⁹ However, other evidence also demonstrated that HG can enhance the odonto/osteogenic differentiation capacity of stem cells from the apical papilla (SCAP) via NF- κ B pathway.²⁰

Existing studies have demonstrated contradictory results on the impacts of glucose on the differentiation potential of MSCs. And the exact influence of HG on DPSCs also remains unclear. The present study aimed to evaluate the effects of HG environments on multiple aspects of DPSCs behavior, including MSCs immunophenotypic property, cell viability, apoptosis, autophagy, and the potential for osteogenic, adipogenic, and neurogenic differentiation. Our findings may provide a more comprehensive view of DPSCs application potential on stem cell therapy and tissue regenerative treatment on diabetic patients.

Materials and methods

Cell culture

Human DPSCs were obtained from Lonza (Basel, Switzerland) (Catalog #PT-5025). DPSCs were cultured with DPSC Basal Medium (Lonza), supplemented with DPSCGM SingleQuots Kit (Lonza) at 37 °C in an atmosphere of 5 % CO₂ incubator. The medium was changed every two to three days. DPSCs were passaged at 80 % confluence using trypsin, the 4–10 generation of the DPSCs were used in the present study.

Cell viability assay

Cell viability was assessed using a cell counting kit (CCK-8, Dojindo, Tokyo, Japan) as described previously.²¹ Briefly, DPSCs (1×10^3 cells/well) were seeded into 96-well plates overnight and then treated with different glucose concentrations (5.5, 11, 22, 33, 55 mM) for 96 h. The original medium was removed, and 10 % of the CCK-8 in the DPSC Basal Medium (Lonza) was added to the cells for 90 min. The absorbance was measured at 450/650 nm using a

spectrophotometer (Spectra Max 190, Molecular Devices, San Jose, CA, USA).

Western blot analysis

Western blot analysis was carried out as previously described.²² In brief, whole cell lysates were harvested in 0.1 ml of RIPA lysis buffer, and then protein concentration was quantified using a BCA protein assay kit (Thermo Fisher Scientific Inc., Waltham, MA, USA). Proteins were separated by 10 % sodium dodecyl sulfate-polyacrylamide gel (SDS-PAGE) and were transferred to polyvinylidene fluoride (PVDF) membrane. Immunoblotting was performed by incubating the PVDF membrane with primary antibody solutions related to apoptosis (pro-caspase-3, cleaved caspase-3, PARP, and cleaved PARP), autophagy (LC3B-I, LC3B-II, autophagy related [ATG]12-ATG5, and sequestosome-1 [p62]), osteogenic differentiation (dentin sialophosphoprotein [DSPP] and dentin matrix acidic phosphoprotein 1 [DMP-1]), adipogenic differentiation (fatty acid synthase [FAS], sterol regulatory element-binding protein 1 [SREBP-1], peroxisome proliferator-activated receptor gamma [PPAR γ], and CCAAT/enhancer binding protein alpha [C/EBP α]), and neurogenic differentiation (neuronal nuclei [Neu N], beta-3 tubulin [β_3 -tubulin], glial fibrillary acidic protein [GFAP], microtubule-associated protein 2 [MAP2], and 2',3'-cyclic-nucleotide 3'-phosphodiesterase [CNPase]) (Cell Signaling Technology, Danvers, MA, USA) at 4 °C overnight, followed by incubation with corresponding horseradish peroxidase (HRP)-conjugated secondary antibodies for 1 h. The immunoreactive proteins were visualized using an enhanced chemiluminescence kit (ECL, Amersham Biosciences, Buckinghamshire, UK) and detected by the luminescent image analyzer (LAS-3000, Fujifilm, Tokyo, Japan).

MSCs immunophenotype analysis

DPSCs surface markers were evaluated by flow-cytometric analysis. Briefly, cells were harvested after stimulation with 5.5 and 33 mM of glucose for 96 h and incubated in 0.5 % bovine serum albumin (BSA) (Gibco, Waltham, MA, USA) solutions with various antibodies (Invitrogen, Waltham, MA, USA), including positive MSCs-associated cell surface cluster of differentiation (CD) markers (CD44-PE, CD73-PE, and CD90-PE) and negative markers (CD31-PE, CD34-PE, and CD45-PE) for 1 h at room temperature in a dark environment. Data was acquired using a flow cytometer (FACSCalibur) and analyzed using CellQuest software (BD Biosciences, San Jose, CA, USA).

Osteogenic differentiation and Alizarin red staining

To investigate the effects of HG on osteogenic differentiation, DPSCs were pretreated with HG (33 mM) for 48 h prior to differentiation medium incubation. The differentiation medium (Human Mesenchymal Stem cell [hMSC] Osteogenic Differentiation Medium BulletKit, Lonza) was replaced every 3 days. Osteogenesis was assessed by Alizarin red staining after 14 days of differentiation.

Cells were gently washed with PBS (Gibco) after removing the differentiation medium. Fix with 4 % formaldehyde at room temperature for 15 min. After removing formaldehyde, wash the cells three times with distilled water. Discard the water and incubate it in a 40 mM Alizarin red staining solution (ARS, Sigma Aldrich, St. Louis, MO, USA) at room temperature for 30 min. Following incubation, replace the staining solution with distilled water and wash four times before proceeding to observation.

Adipogenic differentiation and oil red-O staining

DPSCs were pretreated with HG (33 mM) for 48 h prior to differentiation medium incubation. The differentiation medium (Human Mesenchymal Stem Cell [hMSC] Adipogenic Differentiation Medium BulletKit, Lonza) was replaced every 3 days. Adipogenesis was assessed by oil red-O staining after 35 days of differentiation.

Oil red-O staining solution (Sigma—Aldrich) was prepared by mixing with distilled water at a 3:2 ratio, followed by incubation at room temperature for 30 min and filtration through a 0.22 μ m filter. For staining, cells were first washed with PBS after removing the culture medium and subsequently fixed with 4 % formaldehyde at room temperature for 30 min. Following fixation, formaldehyde was removed, and the cells were rinsed with distilled water. The prepared oil red-O staining solution was then applied, and the cells were incubated at room temperature for 30 min. After staining, the solution was replaced with distilled water, and the cells were washed thoroughly to remove excess stain before microscopic observation.

Neurogenic differentiation of DPSCs

DPSCs were pre-treated with HG (33 mM) for 48 h prior to differentiation medium incubation. The differentiation medium (Mesenchymal Stem Cell Neurogenic Differentiation Medium, PromoCell, Heidelberg, Germany) was replaced every 3 days. Neurogenesis was evaluated by microscopic observation of neural cell morphology after 7 days of differentiation.

Statistical analysis

All data shown represent the mean \pm standard error of the mean (SEM), with a sample size of $n = 3$ for each group. Significant differences among group means were determined via two-tailed Student's t-test and one-way ANOVA followed by a Bonferroni post-hoc test using IBM SPSS Statistics Version 22 (IBMr SPSSr Statistics 22). Statistical significance was accepted when P -values less than 0.05 ($P < 0.05$).

Results

Effects of HG on cell viability, apoptosis, and autophagy in DPSCs

The cell viability was measured using a CCK-8 kit after DPSCs treated with 5.5, 11, 22, 33, and 55 mM of glucose for

96 h, the results demonstrated that cell viability was significantly decreased when treated with the high level of glucose (33 and 55 mM) (Fig. 1A). The levels of apoptosis-related proteins (pro-caspase-3, cleaved caspase-3, PARP, and cleaved PARP) and autophagy-related proteins (LC3B-I, LC3B-II, ATG12-ATG5, and p62) were analyzed by western blot after treating DPSCs with 33 mM glucose for 48 h (Fig. 1B). The quantitative analysis of cleaved caspase-3 (Fig. 1C), cleaved PARP (Fig. 1D), and LC3B-II/LC3B-I (Fig. 1E) were also conducted. Results demonstrated that the protein expression of cleaved caspase-3, cleaved PARP, and LC3B-II/LC3B-I were significantly increased in HG-treated DPSCs compared to the control cells.

Effects of HG on MSCs immunophenotypic property in DPSCs

DPSCs were treated with 5.5 (Fig. 2A) and 33 mM (Fig. 2B) of glucose for 96 h. The MSCs immunophenotypes were assessed by flow cytometry analysis. MSCs markers (CD44, CD73, and CD90) and hematopoietic lineage markers (CD31, CD34, and CD45) were detected. Results showed that high

glucose (33 mM) stimulation did not significantly influence the MSCs immunophenotypic property of DPSCs, which were positive to MSCs-associated surface markers and negative to hematopoietic cell markers.

Effect of HG on osteogenic, adipogenic, and neurogenic differentiation in DPSCs

DPSCs were pretreated with HG (33 mM) for 48 h prior to the incubation of osteogenic, adipogenic, and neurogenic differentiation medium. Osteogenic differentiation was assessed by Alizarin red staining after 14 days of differentiation (Fig. 3A). The quantification of Alizarin red staining was conducted and demonstrated no significant differences between differentiated control and differentiated HG groups (Fig. 3B). Adipogenic differentiation was assessed by oil red-O staining after 35 days of differentiation. Compared to the non-induced and differentiated control group, more pronounced oil red-O staining was observed in the differentiated HG group (Fig. 3C). Neurogenic differentiation was detected by microscopic observation of neural cell morphology after 7 days of differentiation, and

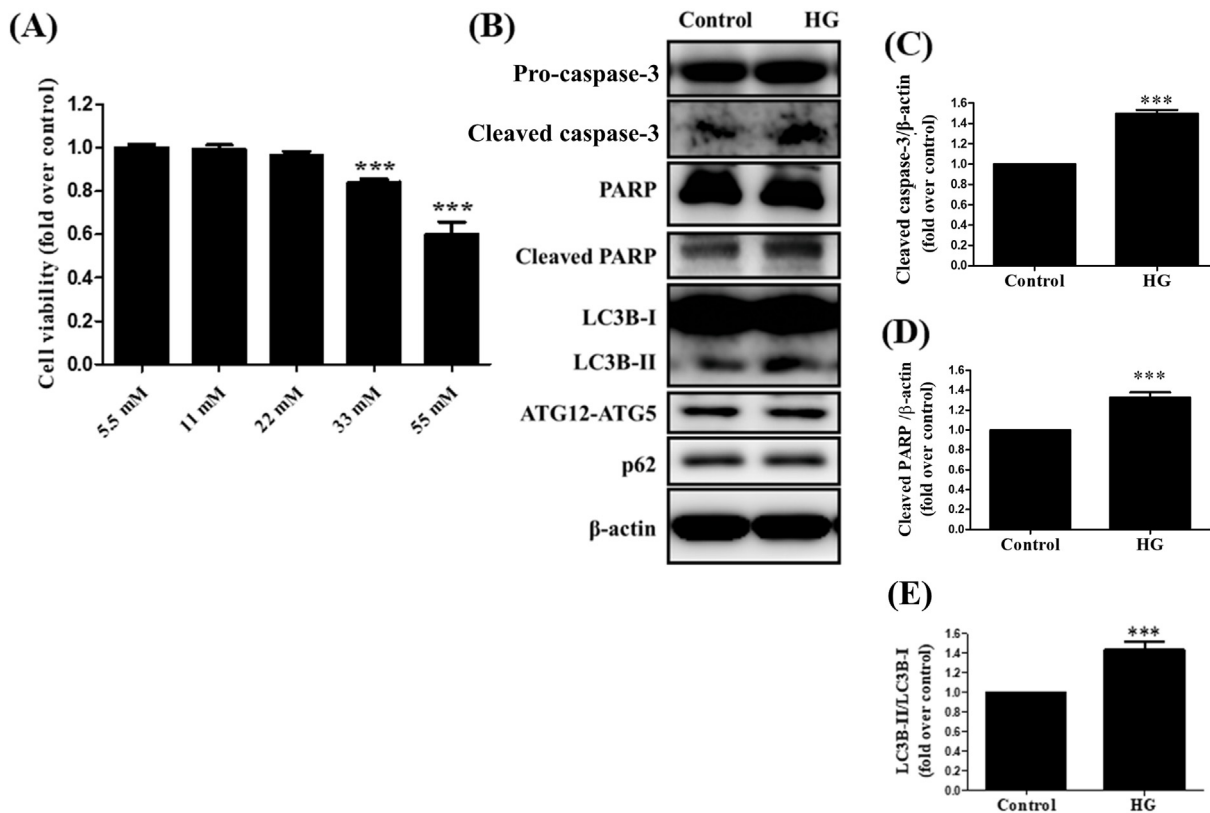


Figure 1 Effects of high glucose on cell viability, apoptosis, and autophagy in DPSCs.

(A) The cell viability was measured using CCK-8 after treating DPSCs with indicated glucose concentrations for 96 h. Results represent the mean \pm SEM ($n = 3$), analyzed via one-way ANOVA followed by a Bonferroni post-hoc test with *** $P < 0.001$ versus 5.5 mM glucose group. (B) The expression of apoptosis-related proteins (pro-caspase-3, cleaved caspase-3, PARP, and cleaved PARP) and autophagy-related proteins (LC3B-I, LC3B-II, ATG12-ATG5, and p62) were analyzed by western blot after 33 mM of high glucose (HG) stimulation for 48 h. The quantitative analysis of cleaved caspase-3 (C), cleaved PARP (D), and LC3B-II/LC3B-I (E) was conducted. Results represent the mean \pm SEM ($n = 3$), analyzed via two-tailed student's t-test with *** $P < 0.001$ versus control. Abbreviation: CCK- cell counting kit, PARP- poly (ADP-ribose) polymerase, LC3B- microtubule-associated protein 1 light chain 3 beta, ATG-autophagy related, p62-sequestosome-1.

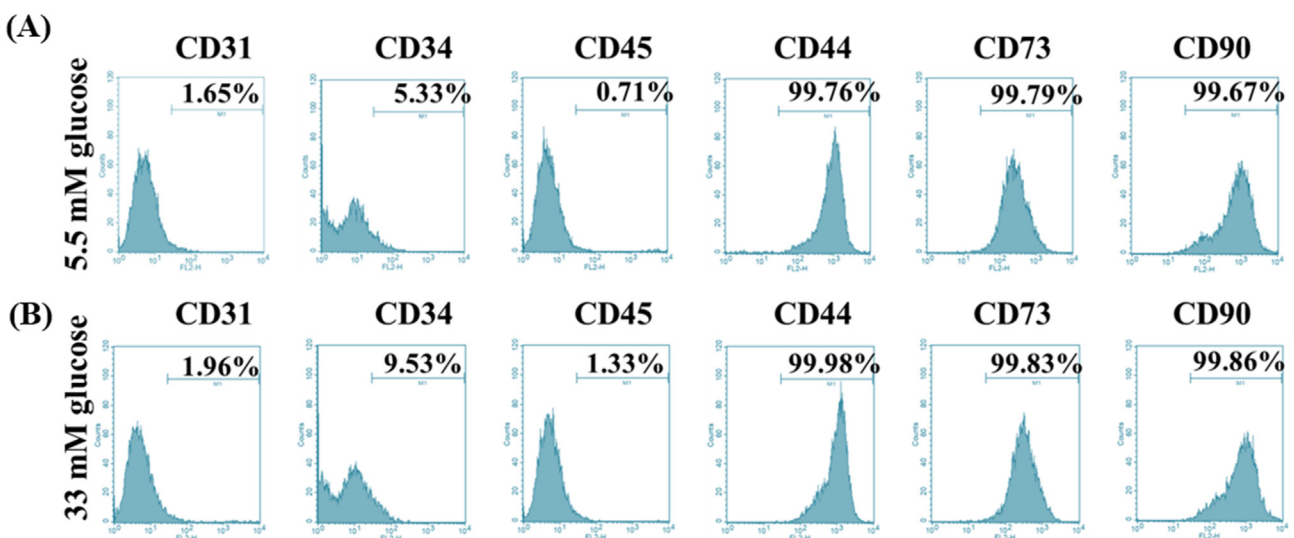


Figure 2 Effects of high glucose on MSCs immunophenotypic property in DPSCs.

DPSCs were treated with 5.5 (A) and 33 mM (B) of glucose for 96 h. The immunophenotypic property was analyzed by flow cytometry. Cluster of differentiation (CD) markers of MSCs (CD44, CD73, and CD90) and hematopoietic stem cells (CD31, CD34, and CD45) were detected.

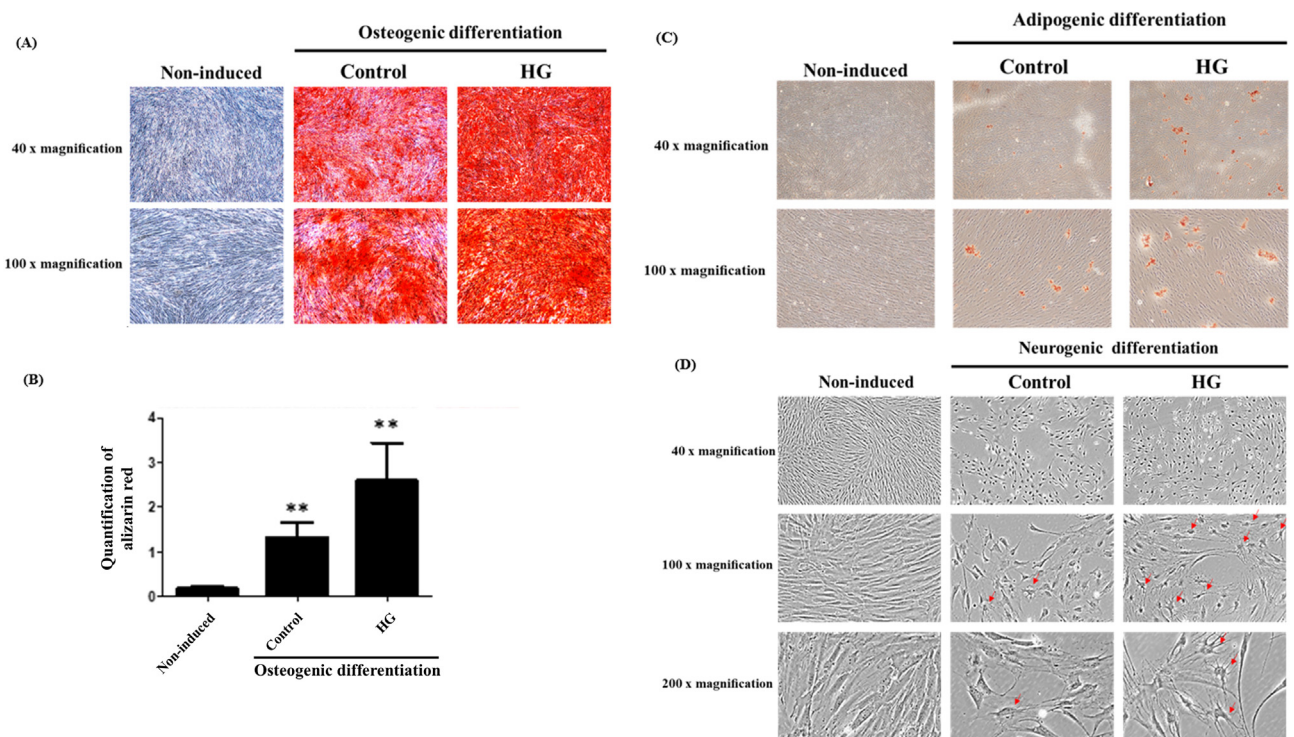


Figure 3 Effect of high glucose on osteogenic, adipogenic, and neurogenic differentiation potential in DPSCs.

DPSCs were pretreated with high glucose (HG) (33 mM) for 48 h prior to differentiation medium incubation. (A) Osteogenic differentiation was assessed by Alizarin red staining after 14 days of differentiation. (B) The quantification of Alizarin red staining was also conducted. Results represent the mean \pm SEM ($n = 3$), analyzed via one-way ANOVA followed by a Bonferroni post-hoc test with $**P < 0.01$ versus control. (C) Adipogenic differentiation was assessed by oil red-O staining after 35 days of differentiation. (D) Neurogenic differentiation was detected by observation of neural-like cell morphology under the microscope after 7 days of differentiation. Multiprocessor neural-like cells were indicated by the red arrows.

the multiprocessor neural-like cells were indicated by the red arrow in Fig. 3D. More multiprocessor neural-like cells in the differentiated HG group were observed compared to the non-induced and differentiated control groups.

The protein expression of osteogenic markers (DSPP and DMP-1) was evaluated by western blot (Fig. 4A), and quantitative analysis of DSPP (Fig. 4B) and DMP-1 (Fig. 4C)

was conducted, results demonstrated that DMP-1 was significantly higher in the differentiated HG group compared to the non-induced and differentiated control groups. Western blotting of adipogenic markers (FAS, SREBP-1, PPAR γ , and C/EBP α) was performed (Fig. 4D). The quantitative analysis results showed no significant changes in the expression of FAS (Fig. 4E), SREBP-1 (Fig. 4F), and

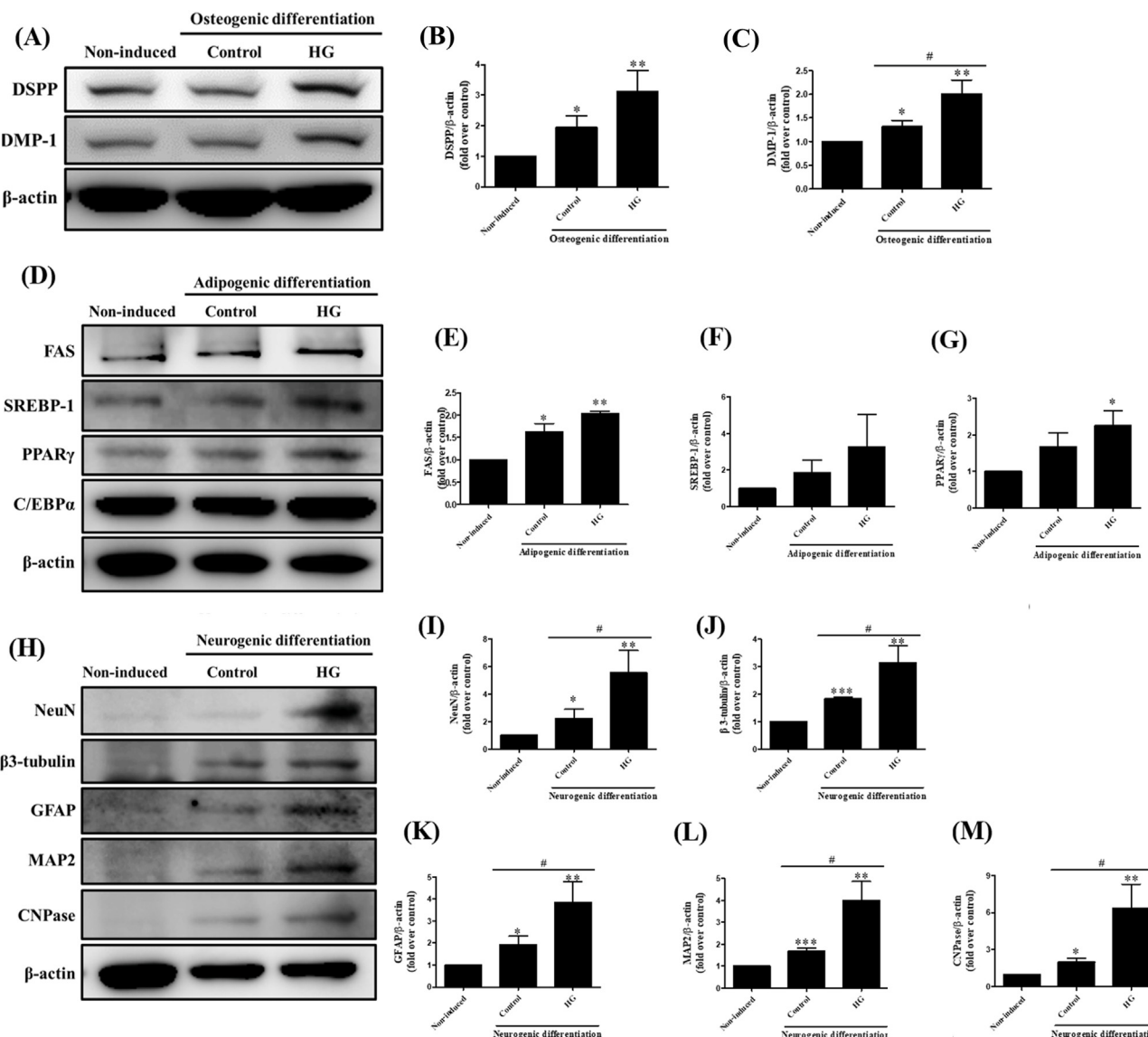


Figure 4 Western blot analysis of the effects of high glucose on the expression of osteogenic, adipogenic, and neurogenic protein in DPSCs.

DPSCs were pretreated with high glucose (HG) (33 mM) for 48 h prior to differentiation medium incubation. (A) The protein expression of osteogenic markers (DSPP and DMP-1) was analyzed by western blot, and the quantitative analysis of DSPP (B) and DMP-1 (C) was conducted. (D) The protein expression of adipogenic markers (FAS, SREBP-1, PPAR γ , and C/EBP α) was analyzed by western blot, the quantitative analysis of FAS (E), SREBP-1 (F), PPAR γ (G) was conducted. (H) Neurogenic markers (NeuN, β 3-tubulin, GFAP, MAP2, and CNPase) were analyzed by western blot, and the quantitative analysis of NeuN (I), β 3-tubulin (J), GFAP (K), MAP2 (L), and CNPase (M) was also conducted. Results represent mean \pm SEM ($n = 3$), analyzed via one-way ANOVA followed by a Bonferroni post-hoc test. * $P < 0.05$, ** $P < 0.01$, and *** $P < 0.001$ versus non-induced control; # $P < 0.05$ versus differentiation control. Abbreviation: DSPP- dentin sialophosphoprotein, DMP-1- dentin matrix acidic phosphoprotein 1, FAS- fatty acid synthase, SREBP-1- sterol regulatory element-binding protein 1, PPAR γ -peroxisome proliferator-activated receptor gamma, C/EBP α - CCAAT/enhancer binding protein alpha, NeuN- neuronal nuclei, β 3-tubulin- beta-3 tubulin, GFAP- glial fibrillary acidic protein, MAP2- microtubule-associated protein 2, CNPase- 2',3'-cyclic-nucleotide 3'-phosphodiesterase.

PPAR γ (Fig. 4G) in the differentiated HG group compared to the differentiated control group. Neurogenic markers (NeuN, β 3-tubulin, GFAP, MAP2, and CNPase) were also evaluated by western blot (Fig. 4H). Results demonstrated that the protein expression of NeuN (Fig. 4I), β 3-tubulin (Fig. 4J), GFAP (Fig. 4K), MAP2 (Fig. 4L), and CNPase (Fig. 4M) was significantly higher in the differentiated HG group compared to the differentiated control group.

Discussion

Stem cells have emerged as a prominent research focus in recent years, particularly in the fields of tissue engineering and regenerative medicine. Notably, dental-derived MSCs, particularly DPSCs, have been utilized in many research due to their multilineage differentiation potential, immunomodulation properties, ease of isolation, etc.²³ It is well established that MSCs require appropriate culture conditions to maintain their cellular and functional properties. Understanding the potential risks in specific cellular environments and optimizing culture conditions are crucial for stem cell therapy outcomes. DM is a metabolic disorder characterized by persistently elevated blood glucose levels. The impact of diabetes on MSCs has gained increasing attention. Studies have demonstrated that MSCs isolated from diabetic patients and those MSCs cultured in HG microenvironments exhibit altered characteristics and functions, potentially leading to decreased viability, proliferation, and differentiation capabilities.^{16,17,24}

According to the World Health Organization (WHO), the expected values for normal fasting blood glucose concentration range from 3.9 mM to 5.6 mM. When fasting blood glucose levels fall between 5.6 mM and 6.9 mM, lifestyle modifications and regular glycemic monitoring are recommended. Diabetes is typically diagnosed when fasting glucose levels exceed 7.0 mM. However, in vitro studies often utilize glucose concentrations that exceed physiological levels to accelerate cellular responses and simulate prolonged exposure to hyperglycemia. The choice of glucose concentration depends on the cell type, as different tissues exhibit varying tolerances to hyperglycemia. For example, studies on retinal ganglion cells and erythrocytes have utilized higher glucose concentrations (45–100 mM), while retinal vascular endothelial cells exhibit molecular changes at lower glucose concentrations (25–50 mM).^{25,26} In this study, we used glucose concentrations ranging from 5.5 to 55 mM to model the effects of hyperglycemia. The results demonstrated that significant effects emerge at 33 mM, suggesting that this threshold may represent a critical point for cellular dysfunction of DPSCs under HG conditions.

Autophagy used to play a biphasic role, while moderate levels of autophagy can be a protective mechanism, prolonged or excessive autophagy can eventually lead to cell death.²⁷ The results of increased cleaved caspase-3, cleaved PARP, and LC3B-II/LC3B-I ratio without significant changes in p62 or ATG12-ATG5 suggest that apoptosis is the dominant process, while autophagy may only mildly activate. This could indicate that in the HG microenvironment, apoptosis is likely the primary mechanism causing cell

death, with autophagy acting as a secondary process that does not cause major alterations in p62 or ATG12-ATG5. These findings are consistent with the general understanding that hyperglycemic conditions can negatively impact cell health and potentially cell death.

Interestingly, the MSCs immunophenotypic properties of the DPSCs were not influenced by HG as assessed by the expression of MSCs-associated surface markers and the absence of hematopoietic cell markers. However, the maintained surface marker expression doesn't necessarily mean MSCs are unaffected, surface marker expression alone may not fully represent MSCs functionality.²⁸ The effects of HG on cell differentiation can be complex and sometimes contradictory in various studies; therefore, we further investigate the differentiation potential in DPSCs under the HG environment. The present study demonstrated that pretreatment with HG prior to exposure to the differentiation medium can enhance the osteogenic, adipogenic, and neurogenic differentiation potential of DPSCs, as evidenced by increased Alizarin red staining, oil red-O staining, and the presence of more neural-like cells, respectively. The protein expression of osteogenic marker (DMP-1) and neurogenic markers (NeuN, β 3-tubulin, GFAP, MAP2, and CNPase) were significantly increased. These findings reveal complex glucose-dependent regulation of cellular differentiation, where high glucose pretreatment appears to enhance specific lineage differentiation potential through mechanisms that require further exploration.

Our findings emphasize the crucial role of optimized culture conditions in enhancing MSCs functionality and therapeutic potential. The demonstrated differentiation potential of DPSCs under HG conditions suggests their promising application potential in stem cell therapy and regenerative medicine for diabetic patients. However, the *in vivo* studies and comparative analysis across different sources of MSCs are necessary to overcome the present study's limitation of focusing on a single cell type.

In conclusion, this study provides insights into the effects of HG conditions on DPSCs, demonstrating significant alterations in their properties and therapeutic potential. Our findings revealed that the HG environment has detrimental effects on cell viability and causes apoptosis while also potentially enhancing the osteogenic, adipogenic, and neurogenic differentiation pathways of DPSCs. These results have important implications for both basic research and future clinical applications in regenerative medicine for diabetic patients.

Declaration of competing interest

The authors have no conflicts of interest relevant to this article.

Acknowledgments

The authors gratefully acknowledge the support of Tri-Service General Hospital (TSGH-A-112010) and the National Taiwan University of Science and Technology (TSGH-NTUST-112-04).

References

1. Fuchs E, Segre JA. Stem cells: a new lease on life. *Cell* 2000; 100:143–55.
2. Martin GR, Evans MJ. Differentiation of clonal lines of teratocarcinoma cells: formation of embryoid bodies in vitro. *Proc Natl Acad Sci U S A* 1975;72:1441–5.
3. Itskovitz-Eldor J, Schuldiner M, Karsenti D, et al. Differentiation of human embryonic stem cells into embryoid bodies comprising the three embryonic germ layers. *Mol Med* 2000;6: 88–95.
4. Nie C, Yang D, Xu J, Si Z, Jin X, Zhang J. Locally administered adipose-derived stem cells accelerate wound healing through differentiation and vasculogenesis. *Cell Transplant* 2011;20: 205–16.
5. Gronthos S, Mankani M, Brahim J, Robey PG, Shi S. Postnatal human dental pulp stem cells (DPSCs) in vitro and in vivo. *Proc Natl Acad Sci U S A* 2000;97:13625–30.
6. Mao JJ, Prockop DJ. Stem cells in the face: tooth regeneration and beyond. *Cell Stem Cell* 2012;11:291–301.
7. Isobe Y, Koyama N, Nakao K, et al. Comparison of human mesenchymal stem cells derived from bone marrow, synovial fluid, adult dental pulp, and exfoliated deciduous tooth pulp. *Int J Oral Maxillofac Surg* 2016;45:124–31.
8. Min Q, Yang L, Tian H, Tang L, Xiao Z, Shen J. Immunomodulatory mechanism and potential application of dental pulp-derived stem cells in immune-mediated diseases. *Int J Mol Sci* 2023;24:8068.
9. Zheng J, Kong Y, Hu X, et al. MicroRNA-enriched small extracellular vesicles possess odonto-immunomodulatory properties for modulating the immune response of macrophages and promoting odontogenesis. *Stem Cell Res Ther* 2020;11:517.
10. Morsczeck C, Reichert TE. Dental stem cells in tooth regeneration and repair in the future. *Expert Opin Biol Ther* 2018;18: 187–96.
11. Graziano A, d’Aquino R, Laino G, Papaccio G. Dental pulp stem cells: a promising tool for bone regeneration. *Stem Cell Rev* 2008;4:21–6.
12. Jamal M, Chogle S, Goodis H, Karam SM. Dental stem cells and their potential role in regenerative medicine. *Hamdan Med J* 2011;4:53–61.
13. Zhou B, Lu Y, Hajifathalian K, et al. Worldwide trends in diabetes since 1980: a pooled analysis of 751 population-based studies with 4.4 million participants. *Lancet* 2016;387: 1513–30.
14. Ampofo AG, Boateng EB. Beyond 2020: modelling obesity and diabetes prevalence. *Diabetes Res Clin Pract* 2020;167:108362.
15. Abu-El-Rub E, Almahasneh F, Khasawneh RR, et al. Human mesenchymal stem cells exhibit altered mitochondrial dynamics and poor survival in high glucose microenvironment. *World J Stem Cell* 2023;15:1093–103.
16. Filion TM, Skelly JD, Huang H, Greiner DL, Ayers DC, Song J. Impaired osteogenesis of T1DM bone marrow-derived stromal cells and periosteum-derived cells and their differential in-vitro responses to growth factor rescue. *Stem Cell Res Ther* 2017;8:65.
17. Chen X, Shen WB, Yang P, Dong D, Sun W, Yang P. High glucose inhibits neural stem cell differentiation through oxidative stress and endoplasmic reticulum stress. *Stem Cell Dev* 2018; 27:745–55.
18. Cheng NC, Hsieh TY, Lai HS, Young TH. High glucose-induced reactive oxygen species generation promotes stemness in human adipose-derived stem cells. *Cytotherapy* 2016;18: 371–83.
19. Khasawneh RR, Abu-El-Rub E, Almahasneh FA, et al. Addressing the impact of high glucose microenvironment on the immunosuppressive characteristics of human mesenchymal stem cells. *IUBMB Life* 2024;76:286–95.
20. Wang Y, Wang Y, Lu Y, Yu J. High glucose enhances the odonto/osteogenic differentiation of stem cells from apical papilla via NF-KappaB signaling pathway. *BioMed Res Int* 2019;2019: 5068258.
21. Chang PK, Yen IC, Tsai WC, Chang TC, Lee SY. Protective effects of Rhodiola crenulata extract on hypoxia-induced endothelial damage via regulation of AMPK and ERK pathways. *Int J Mol Sci* 2018;19:2286.
22. Lin KT, Chang TC, Lai FY, Lin CS, Chao HL, Lee SY. Rhodiola crenulata attenuates gamma-ray induced cellular injury via modulation of oxidative stress in human skin cells. *Am J Chin Med* 2018;46:175–90.
23. Anitua E, Troya M, Zalduendo M. Progress in the use of dental pulp stem cells in regenerative medicine. *Cytotherapy* 2018; 20:479–98.
24. Alicka M, Major P, Wysocki M, Marycz K. Adipose-derived mesenchymal stem cells isolated from patients with type 2 diabetes show reduced “stemness” through an altered secretome profile, impaired anti-oxidative protection, and mitochondrial dynamics deterioration. *J Clin Med* 2019;8:765.
25. Wang Q, Zhang X, Wang K, et al. An in vitro model of diabetic retinal vascular endothelial dysfunction and neuroretinal degeneration. *J Diabetes Res* 2021;2021:9765119.
26. Viskupicova J, Blaskovic D, Galiniak S, et al. Effect of high glucose concentrations on human erythrocytes in vitro. *Redox Biol* 2015;5:381–7.
27. Liu S, Yao S, Yang H, Liu S, Wang Y. Autophagy: regulator of cell death. *Cell Death Dis* 2023;14:648.
28. Boheler KR. Functional markers and the ‘homogeneity’ of human mesenchymal stem cells. *J Physiol* 2004;554:592.